JACS
JOURNAL OF THE AMERICAN CHEMICAL SOCIETY
Article
pubs.acs.org/JACS

Spin-Selective Charge Recombination in Complexes of CdS Quantum Dots and Organic Hole Acceptors

David J. Weinberg,[†] Scott M. Dyar,[†,‡] Zane Khademi,[†] Michał Malicki,[†] Seth R. Marder,[§] Michael R. Wasielewski,[†,‡] and Emily A. Weiss*[,†,‡]

[†]Department of Chemistry and [‡]Argonne-Northwestern Solar Energy Research (ANSER) Center, Northwestern University, 2145 Sheridan Rd., Evanston, Illinois 60208-3113, United States

[§]School of Chemistry and Biochemistry and Center for Organic Photonics and Electronics, Georgia Institute of Technology, 901 Atlantic Drive, Atlanta, Georgia 30332-0400, United States

Supporting Information

ABSTRACT: This paper describes the mechanisms of charge recombination on both the nanosecond and microsecond time scales in a donor−acceptor system comprising thiol-modified bis(diarylamino)4,4′-biphenyl (TPD) molecules attached to a CdS quantum dot (QD) via the thiolate linker. Transient absorption measurements, in conjunction with EPR and magnetic field effect studies, demonstrate that recombination on the nanosecond time scale is mediated by radical pair intersystem crossing (RP-ISC), as evidenced by the observation of a spin correlated radical ion pair, the formation of the localized ^{3}*TPD state upon charge recombination, and the sensitivity of the yield of ^{3}*TPD to an applied magnetic field. These experiments show that the radical spins of the donor−acceptor system have weak magnetic exchange coupling ($|2J| < 10$ mT) and that the electron donated to the QD is trapped in a surface state rather than delocalized within the QD lattice. The microsecond-time scale recombination is probably gated by diffusion of the trapped electron among QD surface states. This study demonstrates that magneto-optical studies are useful for characterizing the charge-separated states of molecule−QD hybrid systems, despite the heterogeneity in the donor−acceptor geometry and the chemical environment of the radical spins that is inherent to these systems.

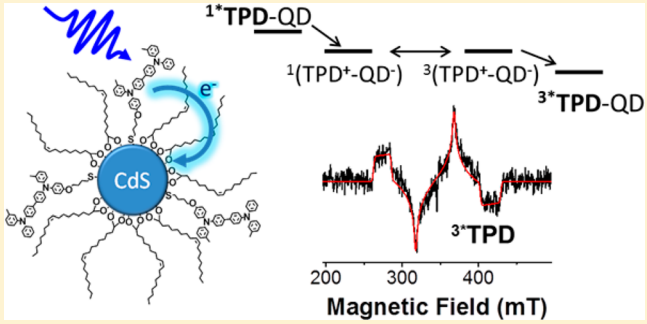

INTRODUCTION

This paper describes two mechanisms by which long-lived charge-separated states recombine within a molecule−quantum dot (QD) donor−acceptor complex: (i) spin-selective recombination of a spin-correlated radical ion pair (RP) on the nanosecond time scale, and (ii) recombination of one carrier on the molecule with a diffusing carrier trapped on the QD surface on the microsecond time scale. The RP is formed by photoexcitation of *N*-[4-(12-mercaptobutyloxy)phenyl]-*N*′-phenyl-*N*,*N*′-di(*m*-tolyl)-biphenyl-4,4′-diamine ("TPD-C4-SH") and subsequent electron transfer to a CdS QD to which the molecule is adsorbed through the thiolate linkage, Figure 1A. Colloidal QDs are photostable, highly absorptive, solution processable charge-transfer partners for organic molecules and polymers.[1−7] In order to use QDs as components of photovoltaic active materials, within which long-lived photogenerated charge pairs are the most likely to be harvested at device contacts,[8,9] we must identify QD−molecule systems in which the rates of charge recombination (after photoinduced electron or hole transfer) are on the nanosecond time scale or longer and determine the mechanisms by which the charge-separated state is preserved.[10] Quantitative mechanistic analyses of charge-transferring systems involving semiconductor nanoparticles are complicated by the chemical and structural heterogeneity of the binding sites on a single QD surface, and the heterogeneity of these surfaces within an ensemble of QDs.[1,5,11] Here, we show that even a heterogeneous ensemble of RPs formed in a QD−molecule system displays behaviors characteristic of RPs in well-defined, geometrically rigid all-organic systems and that the formalism of radical pair spin states developed for these all-organic materials is useful for determining the parameters of the RPs that dictate their lifetime.

Charge separation lifetimes on the nanosecond to microsecond time scales are common in all-organic donor−acceptor systems.[8,9,12−14] For many organic donor−acceptor systems that form RPs with lifetimes of nanoseconds (usually covalently bound multichromophoric molecules),[12,13,15,16] the spins of the radical cation and radical anion are correlated through a nonzero exchange interaction, that is, the RP is in either a net singlet or net triplet state, and these two states interconvert primarily through hyperfine interactions on the respective radical centers, a process called radical pair intersystem crossing

Received: July 18, 2014
Published: September 17, 2014

   dx.doi.org/10.1021/ja507301d | J. Am. Chem. Soc. 2014, 136, 14513−14518

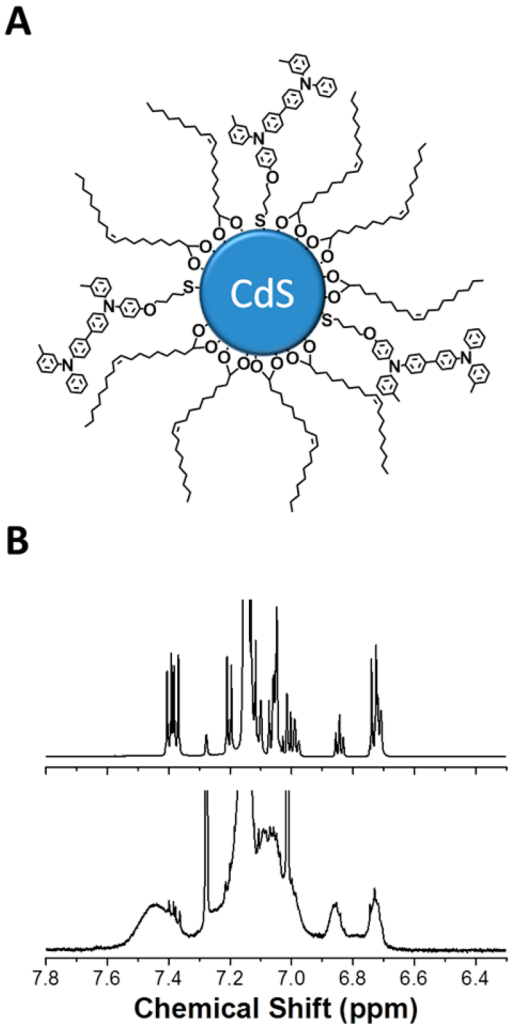

Figure 1. (A) TPD-C4-SH molecules conjugated to CdS QDs with a radius of 0.85 nm. Samples were prepared by treating QDs capped with oleate ligands with a solution of 3 equiv TPD-C4-SH. (B) Comparison of the aromatic region of ^{1}H NMR spectrum of free TPD-C4-SH in d_6-benzene (top) with the ^{1}H NMR spectrum of CdS QDs treated with 3 equiv TPD-C4-SH (bottom). Broadened peaks at 7.44, 7.07, 6.85, and 6.73 ppm correspond to surface-bound TPD-C4-thiolate. The large sharp signals at 7.15, 7.27, and 7.01 ppm correspond to benzene. The remaining sharp peaks (for example, 7.38 ppm) correspond to residual free TPD-C4-SH (~10% of the total population of TPD).

(RP-ISC). The charge recombination of these spin-correlated RPs proceeds through two spin-selective channels: the singlet RP recombines to the singlet ground state of the donor–acceptor complex, and the triplet RP recombines to a localized triplet excited state on one of the chromophores.[12,16−19] Characterizing the spin-correlated RP and the spin-polarized localized triplet that it forms through both transient absorption (TA) and magnetic resonance experiments allows not only calculation of the rate constants for each spin-selective pathway but also estimation of the magnitude of the electronic coupling for electron transfer, the donor–acceptor distance, and the gyromagnetic ratio, g, for each radical spin, which relates to the chemical environment of the radical.[12,18−21] For organic systems that form RPs with lifetimes of microseconds or longer, usually polymeric or self-assembled systems with extended percolation pathways for the electron or hole,[7,12,13] one or both charge carriers migrate so as to at least temporarily lose communication with the other carrier and thus preserve the charge-separated state.[9,15] There are many reports of the use of colloidal QDs as redox centers within solution-phase donor–acceptor systems and within PV active materials, but these reports do not describe charge recombination mechanisms for either of these types of characteristically long-lived RPs.[3−6]

In this work, we characterize the photogenerated RPs formed within a solution-phase ensemble of TPD-CdS QD donor–acceptor systems; these RPs undergo charge recombination on both the nanosecond and microsecond time scales. The RPs that live for ~10 ns recombine spin-selectively to either the singlet ground state or a localized triplet excited state on TPD, ^{3}*TPD. The magnetic field effect (MFE) experiment, a form of optical magnetic resonance, and electron paramagnetic resonance (EPR) experiments confirm that charge recombination dynamics on this time scale are gated by the RP-ISC process, yield a magnetic exchange coupling $|2J|$ of <10 mT (or $<10^{-6}$ eV) for the RP, and indicate that the "acceptor" state of the QD is a surface-localized state rather than a delocalized state of the core. The localization of the electron on the surface of the QD also sometimes results in RPs that live for hundreds of microseconds in this system, due to diffusion of the electron among surface states.

RESULTS AND DISCUSSION

We use a procedure adapted from Evans et al.[22] to synthesize CdS QDs with a band edge absorption peak centered at 328 nm (see the Supporting Information, Figure S1), a radius of 0.85 nm,[23] and coated with oleate ligands. We treat these QDs with 3 equiv of TPD-C4-SH, synthesized using a procedure adapted from Malicki et al.[24] (see the Supporting Information), in d_6-benzene. This sample was prepared under inert atmosphere in order to prevent the oxygen-driven formation of TPD-C4-disulfide. We then determine the number of TPD-C4-SH bound per QD within the mixed monolayer of TPD and oleate, Figure 1A. The ^{1}H NMR spectrum of free TPD-C4-SH has a series of sharp aromatic proton peaks between 6.7 and 7.5 ppm (Figure 1B, top); when TPD-C4-thiolate binds to the surface of a CdS QD, these peaks broaden and shift downfield (Figure 1B, bottom). The lowest field aromatic peak (at 7.44 ppm in the spectrum of QD-TPD mixtures) corresponds to four equivalent protons on the bridging aryl groups. Upon exchange of the native oleate ligands for TPD-C4-SH, the integrated intensity per proton of the peak at 7.44 ppm matches (within 20%) the integrated intensity per proton of the peak at 5.5 ppm corresponding to the vinyl protons of oleic acid that has been displaced by TPD (see the Supporting Information, Figure S2). This result indicates that each TPD-C4-SH displaces a single oleate ligand and that the total ligand count is conserved during the ligand exchange. The ^{1}H NMR spectrum of the mixed monolayer also indicates that 90 ± 5% of TPD-C4-SH present in each sample is bound (see the Supporting Information, Figure S2); we therefore hereafter treat "equivalents TPD-C4-SH added" as "equivalents TPD-C4-SH bound" to the QD.

We next measure the TA spectrum of the TPD-CdS QD complex with three bound TPD molecules per QD using samples that are simply a 2:1 dilution of the NMR samples in toluene. Excitation of the sample at 355 nm results primarily in the formation of ^{1}*TPD (Scheme 1, Step 1), but 20% of absorbed photons excite the QD. Due to the "type-II"

dx.doi.org/10.1021/ja507301d | J. Am. Chem. Soc. 2014, 136, 14513−14518

Scheme 1

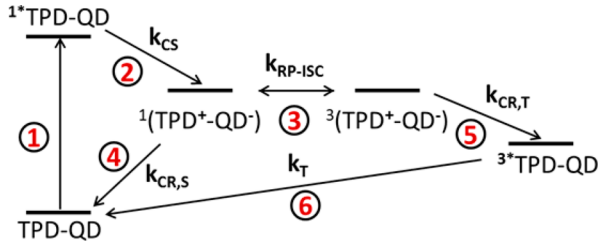

Energy level diagram showing charge separation from the photoinduced singlet excited state of TPD (^{1}*TPD) to form the singlet radical ion pair ^{1}(TPD$^{+\bullet}$-CdS QD$^{-\bullet}$) with rate constant k_{CS}; radical pair intersystem crossing to the triplet radical ion pair ^{3}(TPD$^{+\bullet}$-CdS QD$^{-\bullet}$) with rate constant $k_{RP\text{-}ISC}$; spin-selective recombination from the singlet RP to the singlet ground state with rate constant $k_{CR,S}$; recombination from the triplet RP to the localized triplet excited state of TPD (^{3}*TPD-QD) with rate constant $k_{CR,T}$; and recombination of ^{3}*TPD-QD to the ground state with rate constant k_T

heterojunction formed by this donor–acceptor pair (see the Supporting Information, Figure S3), both excited states yield the same radical pair TPD$^{+\bullet}$-QD$^{-\bullet}$ (Scheme 1, Step 2). The spectral signature of the RP is a prominent absorption feature centered at ∼1450 nm, which corresponds to TPD$^{+\bullet}$.[24,25] Figure 2 shows that the growth of the TPD$^{+\bullet}$ feature at 1450

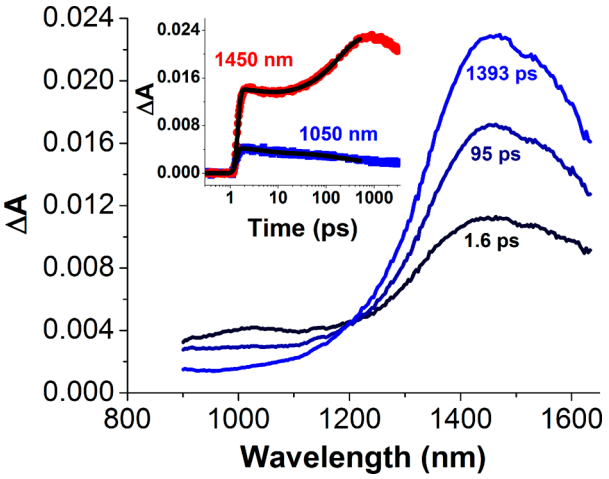

Figure 2. Near-infrared (NIR) TA spectra of a sample of CdS QDs coated with 3 equiv TPD-C4-thiol, in d_6-benzene:toluene, following 355 nm excitation, acquired on the picosecond-to-nanosecond time scale. The sharp feature at 1450 nm corresponds to TPD$^{+\bullet}$. The inset shows kinetic traces extracted from the TA spectrum of the same sample at 1050 nm (blue) and 1450 nm (red). The thin black lines are fits of the data with the IRF convoluted with a sum of two exponential functions, including a charge separation component with τ_{CS} = 201 ps.

nm is concurrent with the decay of the ^{1}*TPD excited-state absorption, which we monitor at 1050 nm based on TA spectra of the free TPD molecule (see the Supporting Information, Figure S4). We do not monitor the dynamics of the QD exciton because our TA spectrometer does not generate sufficient white light at the wavelength of the ground state bleach (328 nm) to accurately measure a transient signal. In order to obtain the charge separation time constant, τ_{CS}, which appears as a decay component at 1050 nm and a rise component at 1450 nm, we globally fit the picosecond kinetic traces at these two wavelengths (Figure 2, inset) to a sum of two simple exponential functions convoluted with an instrument response function (IRF) (see the Supporting Information). This process yields (i) τ_{CS} = 201 ps and (ii) a time constant, τ_1 = 4.2 ps, for decay of ^{1}*TPD due to vibrational relaxation;[24] the τ_1 component is also present at 1450 nm due to nonzero contribution from ^{1}*TPD at this wavelength.

The radical cation feature centered at 1450 nm persists on the nanosecond-to-microsecond time scale, Figure 3A, and exhibits a distinct initial decay in the first hundred nanoseconds after photoexcitation that is followed by a much slower recombination process over the next 400 μs, Figure 3C, red. The initial decay of the TPD$^{+\bullet}$ feature at 1450 nm, which occurs with an 8 ns lifetime, is correlated with the growth of the ^{3}*TPD feature at 633 nm (Figure 3B) with a lifetime of 16 ns (Figure 3C, black). The fact that ^{3}*TPD is produced upon charge recombination of the RP indicates that intersystem crossing must occur between the singlet RP, ^{1}(TPD$^{+\bullet}$-CdS QD$^{-\bullet}$), formed from ^{1}*TPD, and the triplet RP, ^{3}(TPD$^{+\bullet}$-CdS QD$^{-\bullet}$), during its lifetime (Scheme 1, Step 3), because, in general, the recombination of RPs occurs spin-selectively, that is, spin multiplicity is preserved upon charge transfer.[12,15−17,26] The singlet RP, ^{1}(TPD$^{+\bullet}$-CdS QD$^{-\bullet}$), recombines to the neutral singlet ground state of the complex (Scheme 1, Step 4), and ^{3}(TPD$^{+\bullet}$-CdS QD$^{-\bullet}$) recombines to ^{3}*TPD (Scheme 1, Step 5). This type of spin-selective charge recombination only occurs if the RP is spin-correlated rather than two uncoupled radical ions.

In order to confirm the formation of a spin-correlated RP, we conducted transient EPR (TREPR) experiments using continuous microwave irradiation at X-band (9.5 GHz) following pulsed laser photoexcitation of the sample at 355 nm. The room temperature EPR spectrum of the photoexcited TPD-CdS QD complex, Figure 4A (inset), exhibits a broad signal centered at 343 mT, which yields a value for the gyromagnetic ratio g for the spin-correlated radicals of 2.02. This spectrum is consistent with the formation of a spin correlated radical ion pair that originates from a singlet precursor (i.e., ^{1}*TPD) with weak ($|2J| < 10$ mT = $< 10^{-6}$ eV) spin–spin exchange energy.[12,17,18,20] Previous EPR studies of the spin environment of photoinjected carriers in semiconductor nanocrystals show that a g-factor of 2 corresponds to a carrier trapped in a localized state on the QD surface.[11,27−31] If the extra electron on the QD was instead delocalized over a QD core of this size, g would be 1.9 ± 0.05[27,32] as a result of the large spin–orbit interaction of the electron with the full nanocrystal semiconductor lattice,[28,29,33,34] and there would be a signal near 365 mT. We see no signal at 365 mT in Figure 4A (inset) and therefore conclude that all photoinjected electrons are, by 30 ns after photoexcitation (the instrument response time of the EPR experiment), trapped following charge transfer from TPD.[12,17,18] Also, no EPR signal is present at room temperature for CdS QDs treated with 3 equiv of decanethiol rather than TPD-C4-SH following photoexcitation at 355 nm (see the Supporting Information, Figure S5), so electron transfer is necessary to produce this signal.

The EPR spectrum of the photoexcited TPD-CdS QD complex at 85K, Figure 4A, is dominated by the localized triplet state, ^{3}*TPD, with a characteristic dipolar coupling parameter, D, of 835 G. This triplet spectrum fits to a polarization pattern (red) that confirms that it originates primarily from recombination of ^{3}(TPD$^{+\bullet}$-CdS QD$^{-\bullet}$) via the aforementioned RP-ISC mechanism, in which singlet–triplet RP interconver-

dx.doi.org/10.1021/ja507301d | J. Am. Chem. Soc. 2014, 136, 14513−14518

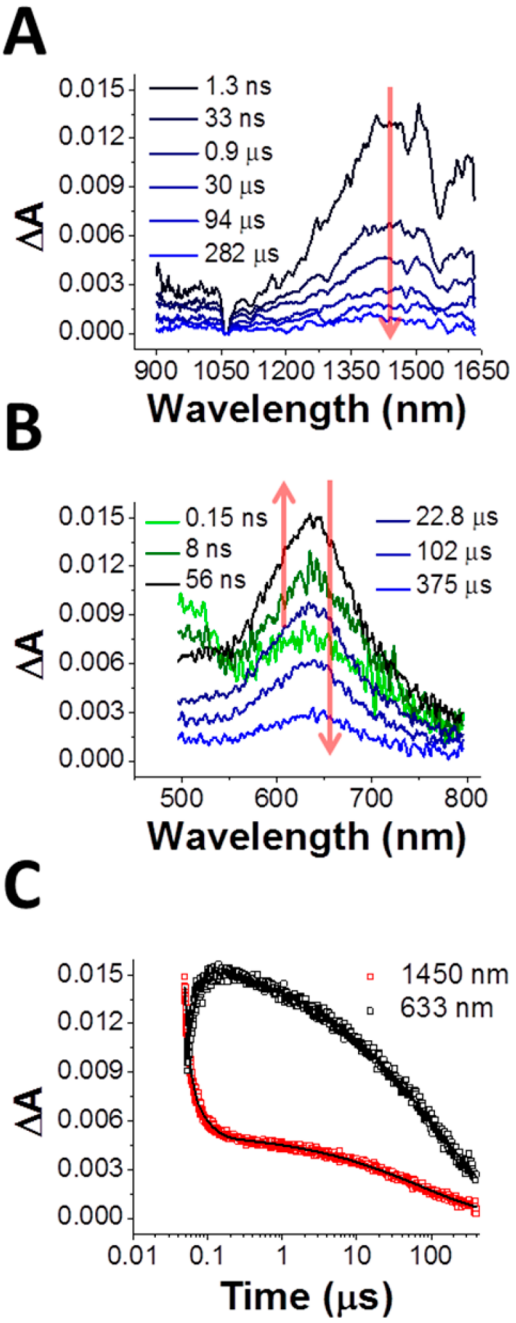

Figure 3. (A) NIR and (B) visible TA spectra of the same sample studied to produce Figure 2 but acquired on the nanosecond-to-microsecond time scale. The feature at 1065 nm in (A) is caused by partial saturation of the detector by the probe. (C) Kinetic traces extracted from the TA spectra in (A) and (B) at 633 nm (black) and 1450 nm (red) showing the dynamics of ^{3}*TPD and TPD$^{+\bullet}$, respectively. The black lines correspond to fits of data to a sum of either one (633 nm) or two (1450 nm) exponentials functions plus a stretched exponential.

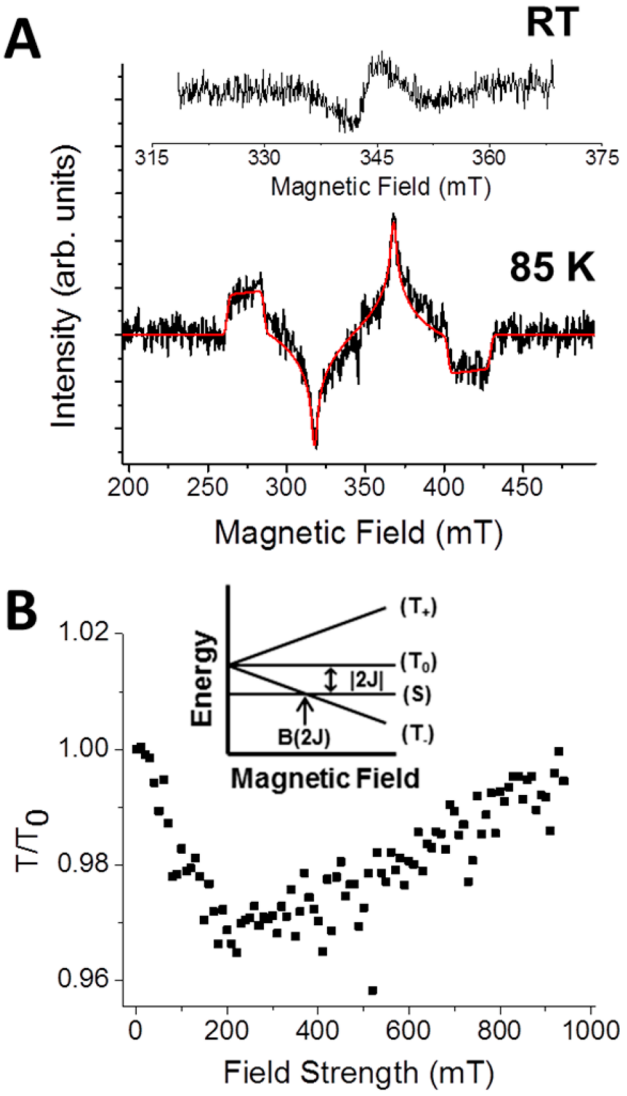

Figure 4. (A) TREPR spectrum of the TPD-CdS QD complex acquired at 85 K at 208 ns after photoexcitation, dominated by the signal of ^{3}*TPD (note the small RP signal centered at 347 mT). The red line is the fit of the low-temperature spectrum based on expected electron spin polarization of ^{3}*TPD following recombination from ^{3}(TPD$^{+\bullet}$-CdS QD$^{-\bullet}$) (Scheme 1, Step 4). The inset shows the TREPR spectrum of same sample recorded at room temperature at the instrument-limited maximum of the signal (116 ns after photoexcitation at 355 nm). (B) Relative yield of ^{3}*TPD ("T/T_0") at 300 ns formed following charge recombination of the TPD$^{+\bullet}$-CdS QD$^{-\bullet}$ RP, as a function of the magnitude of the applied static magnetic field. The sample was excited at 355 nm under inert atmosphere, and the absorption of ^{3}*TPD was monitored at 633 nm. The inset shows a diagram of Zeeman splitting of triplet RP states as a function of applied magnetic field (for an antiferromagnetic exchange energy: $2J < 0$). This splitting accounts for the decrease in T/T_0 between 0 and ~225 mT. The text explains the recovery of T/T_0 at larger field strengths.

sion is induced by electron–nuclear hyperfine coupling.[16,17,35] This fit also includes a smaller (20%) contribution from the localized triplet that forms via spin–orbit intersystem crossing of ^{1}*TPD to ^{3}*TPD.[17]

The slight discrepancy between the observed time constant for decay of the RP (8 ns) at 1450 nm and the time constant for formation of ^{3}*TPD (16 ns) at 633 nm, Figure 3C, is probably due to the overlap of signals at these wavelengths, as the parallel decay kinetics of radical pair recombination via the singlet and triplet pathways should yield identical time constants for the growth of ^{3}*TPD and the decay of the radical pair signal (see the Supporting Information). The signal at 633 nm has contributions from the ~10% free TPD in solution as well as a small amount of ^{3}*TPD formed via intersystem crossing from ^{1}*TPD, and CdS QDs exhibit weak

dx.doi.org/10.1021/ja507301d | J. Am. Chem. Soc. 2014, 136, 14513–14518

intraband transitions with energies which span across the entire NIR region of the spectrum.

We obtain additional information about the spin-correlated $TPD^{+\bullet}$-CdS $QD^{-\bullet}$ RP using the MFE experiment. We excited the TPD-CdS QD complex at 355 nm and monitored, by TA, the yield of ^{3}*TPD produced, that is, the amplitude of the TA spectrum of the complex at 633 nm at a time delay of 300 ns (after recombination is complete), as a function of the magnitude of an applied static magnetic field (B) from 0–1000 mT in steps of 10 mT. We acquired a new baseline (zero field) triplet yield every five magnetic field steps to ensure that our results were not influenced by sample degradation. We denote the triplet yield at zero-field "T_0" and the triplet yield at nonzero field "T", and plot the ratio T/T_0 vs B in Figure 4B.

The plot of T/T_0 vs field strength shows two distinct regimes: a sharp drop in triplet yield to ∼96% of its original value until 225 mT, followed by a gradual rise back to unity. The falloff in triplet yield at low magnetic field strength is characteristic of the RP-ISC mechanism, where the Zeeman interaction of the external field with the three sublevels of $^3(TPD^{+\bullet}$-CdS $QD^{-\bullet})$, T_0, T_+, and T_-, splits the T_+ and T_- sublevels symmetrically around T_0 by an energy equal to $g\beta B$ (Figure 4B, inset).[12,19,36] As the energy gap between the singlet RP state and the T_+/T_- triplet RP states widens, the efficiency of RP-ISC decreases, and the observed yield of ^{3}*TPD decreases. In some covalently bound electron-transferring systems with well-defined donor–acceptor geometries, T/T_0 rises to a peak at the applied magnetic field in which the T_+ or T_- RP level crosses the singlet RP energy level; this peak is called a 2J resonance and its value is equal to the singlet–triplet splitting energy in the unperturbed radical pair (Figure 4B, inset).[12,36] We do not observe such a resonance in our MFE scan, even when we acquire MFE data at high resolution (see the Supporting Information, Figure S6), probably because the magnitude of J is small and the resonance is broadened by the large distribution of donor–acceptor distances; this distribution is due to the conformational motion of the ligand, the heterogeneity of binding sites on the QD surface, and the heterogeneity in chemical environments of the radical anion on the QD surface. It is possible that the magnitude of the MFE (∼5%) is reduced by the spin–orbit coupling of the injected electron and the semiconductor nanocrystal lattice. Spin–orbit coupling on a single radical center, particularly in the presence of a heavy atom, has been shown to quench the magnetic field effect in donor–acceptor systems which undergo charge recombination through the radical pair mechanism, as this interaction induces spin relaxation and washes out the preferential population of radical pair spin sublevels following charge transfer.[37,38] Our EPR results indicate, however, that the injected electron on CdS is trapped in a surface site (likely a Cd ion) and does not experience the full spin–orbit interaction of a carrier delocalized across the full nanocrystal lattice, such that, if the spin–orbit interaction is present, our MFE would not be quenched completely.

The gradual rise in T/T_0 from 225 to 1000 mT (Figure 4B) is characteristic of the so-called "delta g mechanism" most famously observed for RPs within photosynthetic reaction center proteins.[19,36,39] Differences in g-factor on the order of ∼0.001 between the RP electron and hole result in periodic dephasing and rephasing of the transverse spin components, which induces periodic transitions between the T_0 and S states with a frequency that depends on the difference in Larmor frequencies of the electron and hole spins. The Larmor frequency is proportional to gB, so this difference increases linearly with field strength, and, at sufficiently high magnetic fields, this $S–T_0$ mixing dominates the RP-ISC process.[19,40]

In addition to the RPs that recombine on the 10 ns time scale via the RP-ISC mechanism, a portion of the RPs in the TPD-QD system persist on the microsecond time scale. The microsecond dynamics were only adequately fit, that is, the residuals of the fit were symmetric around a center line, with additional stretched exponential components, corresponding, we believe, to the recombination of $TPD^{+\bullet}$ with an electron which hops between localized trap sites on the CdS surface. We chose to fit the 1450 nm kinetic with an additional 40 ns component and a stretched exponential centered at 63 μs, and 633 nm kinetic with an additional stretched exponential centered at 130 μs; the kinetic at 1450 nm fits equally well with one exponential and two stretched exponentials (all fits are summarized in Supporting Information Table S1). Charge-separated states that live for microseconds or longer most often involve electrons and holes that are temporarily decoupled due to migration of one or the other carrier.[8,9,41] We do not believe that the hole in TPD is migrating in this case because there are only three TPD molecules adsorbed per QD, and these molecules are separated by insulating oleate ligands by an average distance of ∼2 nm (we see no evidence of dye aggregation on the surface of the QD, see Supporting Information Figure S7). Following charge transfer and trapping on the QD surface, the localized electron, however, is capable of migrating to other trap sites on the QD surface that are spatially separated from the hole. As a result, the charge-separated state persists for up to hundreds of microseconds and exhibits a distribution of recombination rates. Distributed recombination dynamics due to electron hopping are frequently seen in molecular sensitizer-TiO_2 donor–acceptor systems.[41,42] The decay dynamics at 1450 and 633 nm are complicated further by the overlap of signals from $TPD^{+\bullet}$ and ^{3}*TPD at these wavelengths.

CONCLUSIONS

In summary, we have demonstrated that charge recombination of the photogenerated RP in the TPD-CdS QD donor–acceptor pair is gated by radical pair intersystem crossing on the nanosecond time scale and by the migration of trapped electrons on the surface of the nanocrystal in the microsecond time scale. EPR and magnetic field effect experiments on the spin-correlated RP yield an electron exchange energy, 2J, of $<10^{-6}$ eV and indicate that the electron within the RP is trapped on the surface of the QD. A fraction of these trapped electrons migrate among surface states of the QD and result in RPs that persist for tens of microseconds. Our work indicates that spin-correlated RPs do form in QD–molecule systems in cases where the lifetime of the charge-separated state is sufficiently long to permit RP-ISC (several nanoseconds or longer). The presence of the spin-correlated RP is evident in the sensitivity of its recombination products to application of a magnetic field. In addition to the drop in yield of triplet product with increasing magnetic field characteristic of RP-ISC, the RP in the TPD-QD system displays the gradual increase in triplet yield with application of higher magnetic fields characteristic of slightly different chemical environments of the electron and hole. Even with the heterogeneity in the adsorption geometries and linking chemistries inherent in these systems, magneto-optical characterization of these RPs is useful for determining the parameters that dictate the lifetime of the RP, namely

dx.doi.org/10.1021/ja507301d | J. Am. Chem. Soc. 2014, 136, 14513–14518

average donor−acceptor coupling, and degree of delocalization and chemical environments of the radical spins. This type of information will allow us to develop models for electron transfer in heterogeneous systems that are as quantitatively predictive as those developed for all-organic systems.

■ ASSOCIATED CONTENT

Supporting Information

Details of synthesis, measurements and sample prep; ^{1}H NMR determination of TPD surface coverage; TA control experiments on free TPD in the absence of CdS QD; TA fitting functions and fit parameters; EPR and MFE experimental details and control studies; TPD aggregation studies. This material is available free of charge via the Internet at http://pubs.acs.org.

■ AUTHOR INFORMATION

Corresponding Author

e-weiss@northwestern.edu

Notes

The authors declare no competing financial interest.

■ ACKNOWLEDGMENTS

This work was supported by the U.S. Department of Energy, Office of Science, Basic Energy Sciences, through the Early Career Research Award (award no. DE-SC0003998) to E.A.W and by Chemical Sciences, Geosciences, and Biosciences Division, Office of Basic Energy Sciences, DOE under grant no. DE-FG02-99ER14999 to M.R.W. D.W. is funded by the Department of Energy Office of Science Graduate fellowship program (DOE SCGF), which is administered by ORISE-ORAU under contract no. DE-AC05-06OR23100.

■ REFERENCES

(1) Knowles, K. E.; Peterson, M. D.; McPhail, M. R.; Weiss, E. A. *J. Phys. Chem. C* **2013**, *117*, 10229.
(2) Kamat, P. V. *J. Phys. Chem. C* **2007**, *111*, 2834.
(3) Greenham, N. C.; Peng, X. G.; Alivisatos, A. P. *Phys. Rev. B* **1996**, *54*, 17628.
(4) Kamat, P. V. *J. Phys. Chem. C* **2008**, *112*, 18737.
(5) Anderson, N. A.; Lian, T. Q. *Annu. Rev. Phys. Chem.* **2005**, *56*, 491.
(6) Ren, S. Q.; Chang, L. Y.; Lim, S. K.; Zhao, J.; Smith, M.; Zhao, N.; Bulovic, V.; Bawendi, M.; Gradecak, S. *Nano Lett.* **2011**, *11*, 3998.
(7) Talapin, D. V.; Lee, J. S.; Kovalenko, M. V.; Shevchenko, E. V. *Chem. Rev.* **2010**, *110*, 389.
(8) Clarke, T. M.; Durrant, J. R. *Chem. Rev.* **2010**, *110*, 6736.
(9) Ferguson, A. J.; Kopidakis, N.; Shaheen, S. E.; Rumbles, G. *J. Phys. Chem. C* **2011**, *115*, 23134.
(10) Zhang, Y.; Basel, T. P.; Gautam, B. R.; Yang, X. M.; Mascaro, D. J.; Liu, F.; Vardeny, Z. V. *Nat. Commun.* **2012**, *3*, 1043.
(11) Rajh, T.; Poluektov, O.; Dubinski, A. A.; Wiederrecht, G.; Thurnauer, M. C.; Trifunac, A. D. *Chem. Phys. Lett.* **2001**, *344*, 31.
(12) Wasielewski, M. R. *J. Org. Chem.* **2006**, *71*, 5051.
(13) Gust, D.; Moore, T. A.; Moore, A. L.; Lee, S. J.; Bittersmann, E.; Luttrull, D. K.; Rehms, A. A.; Degraziano, J. M.; Ma, X. C.; Gao, F.; Belford, R. E.; Trier, T. T. *Science* **1990**, *248*, 199.
(14) Gust, D.; Moore, T. A.; Moore, A. L. *Acc. Chem. Res.* **2001**, *34*, 40.
(15) Bullock, J. E.; Carmieli, R.; Mickley, S. M.; Vura-Weis, J.; Wasielewski, M. R. *J. Am. Chem. Soc.* **2009**, *131*, 11919.
(16) Carbonera, D.; Di Valentin, M.; Corvaja, C.; Agostini, G.; Giacometti, G.; Liddell, P. A.; Kuciauskas, D.; Moore, A. L.; Moore, T. A.; Gust, D. *J. Am. Chem. Soc.* **1998**, *120*, 4398.
(17) Dance, Z. E. X.; Mi, Q. X.; McCamant, D. W.; Ahrens, M. J.; Ratner, M. A.; Wasielewski, M. R. *J. Phys. Chem. B* **2006**, *110*, 25163.
(18) Hore, P. J.; Hunter, D. A.; Mckie, C. D.; Hoff, A. J. *Chem. Phys. Lett.* **1987**, *137*, 495.
(19) Steiner, U. E.; Haas, W. *J. Phys. Chem.* **1991**, *95*, 1880.
(20) Norris, J. R.; Morris, A. L.; Thurnauer, M. C.; Tang, J. *J. Chem. Phys.* **1990**, *92*, 4239.
(21) Dubinski, A. A.; Perekhodtsev, G. D.; Poluektov, O. G.; Rajh, T.; Thurnauer, M. C. *J. Phys. Chem. B* **2002**, *106*, 938.
(22) Evans, C. M.; Love, A. M.; Weiss, E. A. *J. Am. Chem. Soc.* **2012**, *134*, 17298.
(23) Yu, W. W.; Qu, L. H.; Guo, W. Z.; Peng, X. G. *Chem. Mater.* **2003**, *15*, 2854.
(24) Malicki, M.; Hales, J. M.; Rumi, M.; Barlow, S.; McClary, L.; Marder, S. R.; Perry, J. W. *Phys. Chem. Chem. Phys.* **2010**, *12*, 6267.
(25) Matis, M.; Rapta, P.; Lukes, V.; Hartmann, H.; Dunsch, L. *J. Phys. Chem. B* **2010**, *114*, 4451.
(26) Mclauchlan, K. A.; Steiner, U. E. *Mol. Phys.* **1991**, *73*, 241.
(27) Baranov, P. G.; Orlinskii, S. B.; Donega, C. D.; Schmidt, J. *Appl. Magn. Reson.* **2010**, *39*, 151.
(28) Liu, W. K.; Whitaker, K. M.; Smith, A. L.; Kittilstved, K. R.; Robinson, B. H.; Gamelin, D. R. *Phys. Rev. Lett.* **2007**, *98*, 186804.
(29) Whitaker, K. M.; Ochsenbein, S. T.; Polinger, V. Z.; Gamelin, D. R. *J. Phys. Chem. C* **2008**, *112*, 14331.
(30) Lifshitz, E.; Glozman, A.; Litvin, I. D.; Porteanu, H. *J. Phys. Chem. B* **2000**, *104*, 10449.
(31) Hayoun, R.; Whitaker, K. M.; Gamelin, D. R.; Mayer, J. M. *J. Am. Chem. Soc.* **2011**, *133*, 4228.
(32) Sirenko, A. A.; Belitsky, V. I.; Ruf, T.; Cardona, M.; Ekimov, A. I.; Trallero-Giner, C. *Phys. Rev. B* **1998**, *58*, 2077.
(33) Rodina, A. V.; Efros, A. L.; Alekseev, A. Y. *Phys. Rev. B* **2003**, *67*, 155312.
(34) van Schooten, K. J.; Huang, J.; Baker, W. J.; Talapin, D. V.; Boehme, C.; Lupton, J. M. *Nano Lett.* **2013**, *13*, 65.
(35) Wasserman, E.; Yager, W. A.; Snyder, L. C. *J. Chem. Phys.* **1964**, *41*, 1763.
(36) Chidsey, C. E. D.; Roelofs, M. G.; Boxer, S. G. *Chem. Phys. Lett.* **1980**, *74*, 113.
(37) Levin, P. P.; Kuzmin, V. A. *Chem. Phys. Lett.* **1990**, *165*, 302.
(38) Khudyakov, I. V.; Serebrennikov, Y. A.; Turro, N. J. *Chem. Rev.* **1993**, *93*, 537.
(39) Boxer, S. G.; Chidsey, C. E. D.; Roelofs, M. G. *J. Am. Chem. Soc.* **1982**, *104*, 1452.
(40) Steiner, U. E.; Ulrich, T. *Chem. Rev.* **1989**, *89*, 51.
(41) Hilgendorff, M.; Sundstrom, V. *J. Phys. Chem. B* **1998**, *102*, 10505.
(42) Ghosh, H. N.; Asbury, J. B.; Weng, Y. X.; Lian, T. Q. *J. Phys. Chem. B* **1998**, *102*, 10208.